Journal of Thermal Science Vol.31, No.6 (2022) 1853−1867

**https://doi.org/10.1007/s11630-022-1597-6** **Article ID: 1003-2169(2022)06-1853-15**

# Construction and Optimization of Liquefied Natural Gas Regasification Cold Energy Comprehensive Utilization System on Floating Storage Regasification Unit

**YAO Shouguang[1*], WANG Mengdi[1], YAN Likun[1], ZHANG Qiang[1], YE Yong[2]**

1. School of Energy and Power Engineering, Jiangsu University of Science and Technology, Zhenjiang 212100, China
2. China Ship Shenghui Equipment Co., Ltd, Zhangjiagang 215600, China



**Abstract:** In this paper, the efficient utilization of liquefied natural gas (LNG) vaporization cold energy in offshore liquefied natural gas floating storage regasification unit (FSRU) is studied. On the basis of considering different boil-off gas (BOG) practical treatment processes, a cascade comprehensive utilization scheme of cold energy of LNG based on the longitudinal three-stage organic Rankine cycle power generation and the low-grade cold energy used to frozen seawater desalination was proposed. Through the comparative analysis of the effects of the pure working fluid and eight mixed working fluids on the performance of the new system, the combination scheme of system mixed working fluid with the highest exergy efficiency of the system was determined. Then, the genetic algorithm was used to optimize the parameters of the new system. After optimization, the net output power of the LNG cold energy comprehensive utilization system proposed in this paper was 5186 kW, and the exergy efficiency is 30.6%. Considering the power generation and freshwater revenue, the annual economic benefit of the system operating is 18.71 million CNY.

**Keywords: LNG, cold energy utilization, mixed working fluid, organic Rankine cycle, boil-off gas (BOG) treatment**

## 1. Introduction

As a kind of clean energy with high calorific value and low pollution, natural gas is being used more and more widely [1]. Since natural gas needs to be converted into a low-temperature liquid form for storage and transportation, liquefied natural gas (LNG) must undergo a re-vaporization process before reaching the terminal of the customer, usually using seawater or other waste heat sources as heating sources. If the cold energy is not recycled in the process of LNG vaporization, it will not only cause huge waste of cold energy, but also have a negative impact on the environment [2].

At present, the increasing use of LNG on land has prompted many researchers to study the recovery and utilization of LNG vaporization cold energy. The terminal vaporization of LNG on land mainly occurs in the LNG vaporization plants or stations, and the corresponding cold energy utilization method has been air separation, low temperature crushing, power generation, seawater desalination and refrigeration [3, 4]. Considering that electricity is the most commonly used and convenient secondary energy, and it is less affected by environment, market, traffic and other factors, LNG

Special column: Built Thermal Environment GE: ZHAI Zhiqiang
Received: Jan 13, 2021 Corresponding author: YAO Shouguang E-mail: zjyaosg@126.com

**Nomenclature**

| | | | |
|---|---|---|---|
| BOG | Boil-off Gas | LNGPP | Liquefied natural gas pump |
| D | Seawater desalination flow | ORC | Organic Rankine Cycle |
| DCR | Deep cooler | PCR | Precooler |
| DEQ | Desalination equipment | S | Second working fluid flow |
| F | First working fluid flow | SW | Seawater |
| FSRU | Floating Storage Regasification Unit | T | Third working fluid flow |
| L | LNG working fluid state | TB | Turbine |
| LHEX | LNG heat exchanger | WFPP | Working fluids pump |
| LNG | Liquefied Natural Gas | WHEX | Working fluids heat exchanger |

cold energy generation is generally considered as an efficient way of energy utilization. Reported LNG cold energy power generation technologies includes direct expansion method [5], combined cycle method [6], Brayton cycle method [7], Karina cycle method [8], Rankine cycle method [9] and multi-stage compound cycle method. Among them, the organic Rankine cycle (ORC) power generation method based on low-boiling-point organic matter is the most widely used method [10].

In order to further improve the performance of LNG cold energy power generation system, Bao et al. [11, 12] has successively proposed a two-stage condensation Rankine cycle and a three-stage condensation Rankine cycle for the problem of poor temperature matching between single-stage Rankine cycle working fluid and LNG. Compared with single-stage ORC, the difference between evaporation temperature and condensation temperature of each stage of three-stage Rankine cycle is reduced, making the heat exchange curve of heat exchanger more match, and the system performance is greatly improved. In order to further improve the utilization efficiency of LNG cold energy, some scholars [13–15] combined LNG cold energy power generation with seawater desalination, air separation and other cold energy utilization methods based on the principle of cascade utilization, and proposed a comprehensive utilization system of LNG cold energy. The results show that compared with a single cold energy utilization scheme, the new cold energy comprehensive utilization scheme is more efficient. At the same time, some scholars have found that the energy recovery and utilization efficiency of the LNG cold energy utilization system is not only related to the design of the system process structure, but also influenced by the choice of working fluid [16]. Zhang et al. [17] proposed a combined cycle by three single-stage Rankine cycles in series-parallel, in which industrial waste heat was used as heat source and LNG as the heat sink. They found that the net power output of the system was the largest when the working fluid was n-pentane. Sun et al. [18] studied the effects of pure working fluid and three hydrocarbon mixed working fluids on their power generation performance around a horizontal three-stage Rankine cycle system, and found that a mixture of three hydrocarbons as working fluids can achieve higher efficiency. However, the above researches on cold energy utilization of LNG are all conducted in onshore LNG receiving plants or stations.

With the widespread use of LNG, due to the safety and economic considerations of LNG storage and vaporization, more and smaller emerging markets no longer spend a lot of money to build large-scale onshore regasification facilities, but instead choose to build coastal floating storage regasification unit (FSRU) to receive and process imported LNG. Compared with the traditional LNG receiving and regasification plant model, the FSRU, similar to LNG carrier, can not only transport and store LNG, but also complete regasification of LNG and directly transport natural gas to land end users. It is not only more flexible and convenient to select mooring location, but also relatively cost-effective. However, because FSRU needs to be moored in coastal areas for a long time and is greatly affected by wind, waves and currents, its environmental sensitivity is quite different from that of conventional onshore receiving system. There are obvious differences in the environment and demand between the recovery and utilization of re-vaporization cold energy on FSRU and the traditional onshore LNG vaporization plants. At present, studies on the utilization of regasification cold energy of LNG on FSRU are still very few [19, 20]. Lee [21] studied the effects of pure ethane, pure propane, and mixed working fluid of ethane and propane on the horizontal secondary Rankine cycle based on the LNG-FSRU platform. It was found that when the ratio of ethane and propane was 8: 2, the system exergy loss was the smallest. Zhang et al. [22] focused on the utilization of cold energy in the regasification of LNG-FSRU, and proposed a cascade cold energy utilization system including air separation, dry ice manufacturing, horizontal two-stage Rankine cycle power generation and air-conditioning cold storage. However, this cold energy utilization system does not consider the actual environment and conditions of FSRU,

and the design is too complex and difficult to implement on FSRU. In particular, the LNG storage and regasification environment on FSRU is different from that of onshore gasification installations, which produce a large amount of boil-off gas (BOG) and require disposal for recovery. However, according to the literature retrieved by the author, the research on BOG is all concentrated on a single BOG processing system [23, 24], and the research on combining it with the LNG cold energy utilization system for comprehensive energy utilization has not been reported.

Aiming at the characteristics of limited environment space and large amount of BOG on FSRU, which are different from the LNG storage and vaporization plants on land, this paper studies a FSRU platform with 175 t/h LNG vaporization volume. Considering different actual processing technologies of BOG, as well as the practical and feasible scheme that low-grade cold energy can be used in seawater desalination by freezing method in the later stage of LNG vaporization, a comprehensive utilization scheme of LNG vaporization cold energy under special environment of FSRU is constructed. Based on the thermodynamic analysis of the constructed system, the optimization of the new system is studied from the aspects of process layout, working fluid matching selection and system parameter matching. The optimal technical scheme can provide a good reference for the design of LNG cold energy utilization system on FSRU in the future.

## 2. Proposal and Analysis of Initial System Scheme

Aiming at the characteristics of large LNG vaporization and rich high-grade cold energy on the FSRU, in the early stage of the author's study found that the temperature range of LNG cold energy recovered by single-stage or two-stage organic Rankine cycle is small, so it is difficult to maximize the recovery of LNG high-grade cold energy. Therefore, in order to make full use of LNG vaporized cold energy under supercritical pressure on FSRU, the author previously proposed a single-split longitudinal three-stage organic Rankine cycle power generation system with compact structure and high efficiency recovery of LNG cold energy within a large temperature difference range [19, 20]. However, the new system has not considered the recovery of large amount of BOG on FSRU and the utilization of low-grade cold energy of LNG. Based on the original high-grade cold energy power generation scheme, this paper further adds desalination system to achieve the purpose of recovering LNG low-grade cold energy. At the same time, combined with BOG treatment process, a new LNG cold energy comprehensive utilization system scheme is formed: BOG recondensation LNG cold energy comprehensive utilization system. The detailed flow chart of the new system scheme is shown in Fig. 1.

As can be seen from Fig. 1, the new system scheme consists of three parts. The core part is the single-split longitudinal three-stage organic Rankine cycle for generate electricity, of which only the third stage cycle uses seawater as heat source. Its second stage cycle uses the third stage cycle heat release to provide heat source, and the first stage cycle uses the second stage cycle heat release to provide heat source, which can make full use of the temperature difference between seawater and LNG to generate electricity and reduce the exergy loss. In the initial simulation process, it is found that the heat exchange exergy loss of LNG heat exchanger 3 (LHEX3) is too large, and the temperature difference between LNG

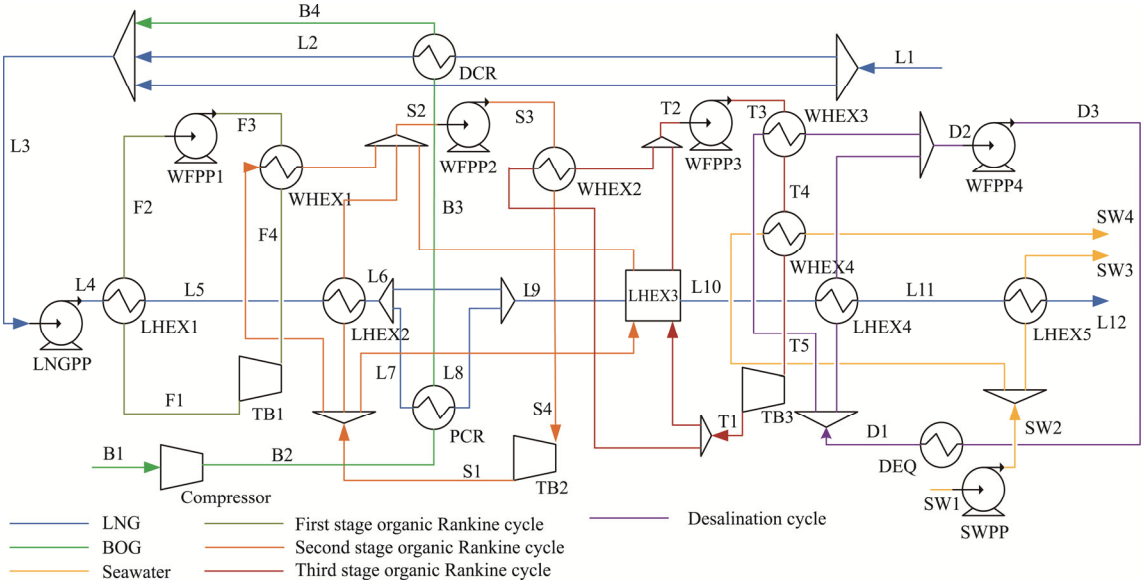


**Fig. 1** Flow chart of new system scheme

and the third stage organic Rankine cycle working fluid is too large. Therefore, it is considered to introduce the second stage organic Rankine cycle working fluid into LHEX3 on the original basis, so as to reduce the heat exchange exergy loss of LHEX3. The seawater desalination part of the new system scheme adopts the direct freezing method to recover the LNG low-grade cold energy. The low-grade cold energy is recovered from LHEX4 and working fluids heat exchanger 4 (WHEX4) by using the intermediate medium, and then in DEQ, seawater is frozen by the intermediate medium to separate and produce fresh water. According to the actual BOG processing process which can be selected on FSRU, the BOG processing part in initial system scheme adopts the recondensation scheme, which uses a multi-stage condensing process to re-liquefy the BOG. BOG is first pressurized by a compressor, then precooled by precooler PCR, and then liquefied by initial LNG in deep cooler (DCR), and finally mixed with liquefied natural gas into power generation and seawater desalination systems.

### 2.1 Simulation initial parameter setting

The initial parameters of the new system scheme are set as follows.

The LNG flow rate is 175 000 kg/h, and the pressure after gasification is 8 MPa;

The LNG component is 95% methane, 3% ethane, 2% propane;

The evaporation of BOG is calculated as 5% of LNG gasified [25];

The initial circulating working fluid condensing pressure is taken as 110 kPa;

The minimum end difference of all heat exchangers is 5°C, and the outlet super-cooling degree of heat flow working fluid is 2°C.

The working fluid state of the inlet of the turbine is saturated gas;

The turbine expander efficiency is 80%, and the pump efficiency is 75%, ignoring all heat exchanger pressure losses;

The seawater temperature is 20°C, and the ambient temperature is 25°C;

The crystallization load $Q$ required for seawater desalination is simulated by Aspen HYSYS, and then the seawater flow and freshwater flow are calculated by the following Eq. (1).

$$Q = m_{\text{seawater}} c\Delta t + m_{\text{ice}}\gamma \tag{1}$$

where, $Q$ is crystallization load; $m_{\text{seawater}}c\Delta t$ is a load of seawater cooling to the freezing point; $m_{\text{ice}}\gamma$ is the seawater crystallization load; $c$ is the specific heat capacity of seawater; $\Delta t$ is the temperature drop in seawater cooling; $\gamma$ is the ice melting heat.

System exergy efficiency:

$$\eta_{\text{nx}} = \frac{W_{\text{net}}}{Ex_{\text{LNG}} + Ex_{\text{seawater}}} \tag{2}$$

where, $W_{\text{net}}$ is system net output work (Since the seawater desalination amount and the turbine output power are two kinds of properties, it is impossible to directly compare them. Here, the revenue of seawater desalination per ton is converted into a power generation of 9 kW [26]). The generator efficiency, which is the output electricity power of the generator and the input power of the shaft end, takes 0.96. $Ex_{\text{LNG}}$ is the exergy of LNG entering the system, and $Ex_{\text{seawater}}$ is the exergy of seawater entering the system.

### 2.2 System working fluid selection

Considering the amount of LNG cold energy released on the FSRU and the cascade matching of LNG cold energy release and recovery, the selection of working fluid is very important. A set of matching working fluid can effectively reduce the loss of cold energy and improve the efficiency of cold energy utilization.

The condensation temperature of common working fluid under 110 kPa is shown in Table 1.

**Table 1** Condensation temperature of common working fluid under 110 kPa

| Working fluid | Condensation temperature | Working fluid | Condensation temperature |
|---|---|---|---|
| R1150 | –102.6°C | R290 | –40.55°C |
| R170 | –87.22°C | R717 | –31.44°C |
| R23 | –80.53°C | R134a | –24.24°C |
| R116 | –77.20°C | R152a | –22.61°C |
| R1270 | –46.16°C | R600a | –9.93°C |
| R143a | –45.38°C | | |

Because the natural gas cold energy used for desalination of seawater only needs the lower grade cold energy at higher temperature, the initial natural gas temperature of LHEX3 outlet for further desalination is considered to be around –45°C. Considering that the selection of two working media in the heat exchanger should meet the minimum end difference of 5°C, the working fluid whose condensation temperature on 110 kPa close to –40°C is R290, R143a and R1270, and R143a is not considered due to its high global warming potential. When R290 is used as the third stage cycle working fluid, the temperature range from LHEX1 inlet to LHEX3 outlet in LNG cold energy power generation system is in the range of –158°C and –45.55°C. It can be seen from Table 1 that the first stage organic Rankine cycle working fluid that meets the conditions is R1150 and R170, and the second stage organic Rankine cycle working fluid that meets the conditions is R23, R116, and R1270. When R1270 is used as the third stage circulating

working fluid, the temperature from LHEX1 inlet to LHEX3 outlet in LNG cold energy power generation system is in the range of –158°C and –51.16°C. The first stage organic Rankine cycle working fluids that meets the conditions are R1150, R170, and the second stage organic Rankine cycle working fluids that meets the conditions are R23, R116. Because R116 belongs to fluoride, it will not be considered here. The selection of working fluid for desalination requires that its evaporation temperature is close to and lower than the seawater freezing point, and its solidification temperature is lower than –45°C (ensure that the desalination working fluid will not solidify during heat exchange with low temperature LNG). By analyzing the physical properties of common refrigerants, R600a is the best working fluid for seawater desalination. The specific combination scheme is shown in Table 2.

**Table 2** Working fluid matching scheme

| Working fluid combination | First stage working fluid | Second stage working fluid | Third stage working fluid | Desalination working fluid |
|---|---|---|---|---|
| Scheme 1 | R1150 | R23 | R1270 | R600a |
| Scheme 2 | R1150 | R23 | R290 | R600a |
| Scheme 3 | R1150 | R1270 | R290 | R600a |
| Scheme 4 | R170 | R23 | R1270 | R600a |
| Scheme 5 | R170 | R23 | R290 | R600a |
| Scheme 6 | R170 | R1270 | R290 | R600a |

In HYSYS, simulation calculations are performed for different scheme of working fluid combination in Table 2. The fluid properties package is Peng-Robinson. The net output power of the system is shown in Supplementary Fig. S1. The working fluid dryness of the three turbine outlets under each scheme of working fluid combination is shown in Supplementary Fig. S2.

From Supplementary Fig. S1, it can be found that when working fluid combination Scheme 2 (R1150, R23, R290, R600a) is used, the new system scheme can reach the maximum net output power, which is 4961 kW. From Supplementary Fig. S2, the dryness of working fluid combination Schemes 4, 5 and 6 is relatively good, but the net output power of the system is relatively low, while the working fluid dryness at the outlet of turbine 1 in the working fluid combination Scheme 3 is 0.892, which is easy to erode the turbine blades. The net output power of Scheme 1 is less than Scheme 2, and the dry degree of working fluid at the outlet of turbine 3 is also lower than Scheme 2. The working fluid dryness at the outlet of each turbine in Scheme 2 is 0.957, 0.940 and 0.998 respectively, which can ensure safety operation of the turbine. Combined with the net output power of each working fluid combination scheme, working fluid combination Scheme 2 (R1150, R23, R290, R600a) should be the preferred working fluid combination scheme.

### 2.3 Simulation results and analysis

Table 3 gives a comparison of the original power generation system and the new system.

**Table 3** Comparison of original and new system schemes

| Programme | Original system [20] | | New system | |
|---|---|---|---|---|
| Module | Exergy loss/kW | Exergy efficiency | Exergy loss/kW | Exergy efficiency |
| Organic Rankine cycle power generation | 13 240 | 23.77% | 11070 | 25.32% |
| Seawater desalination | – | – | 1173 | 48.10% |
| BOG processing | – | – | 461 | 83% |
| LHEX1 | 3266.63 | 65.9% | 2310.02 | 70.5% |
| LHEX2 | 624.70 | 79.7% | 653.24 | 79.9% |
| LHEX3 | 1564.06 | 70.9% | 1771.92 | 68.5% |
| LHEX4 | – | – | 801.65 | 53.8% |
| LHEX5 | 1649.66 | 13.1% | 16.69 | 94.0% |
| WHEX1 | 435.94 | 91.9% | 360.57 | 92.4% |
| WHEX2 | 809.39 | 85.1% | 678.86 | 86.1% |
| WHEX3 | 1302.39 | 38.9% | 1813.61 | 37.6% |
| WHEX4 | – | – | 369.28 | 60.9% |
| TB1 | 277.64 | 69.6% | 239.74 | 69.9% |
| TB2 | 718.92 | 72.1% | 696.72 | 70.7% |
| TB3 | 1403.66 | 75.7% | 1411.5 | 75.3% |
| System total exergy loss/kW | 13 240 | | 12 704 | |
| System net output power/kW | 4130 | | 4961 | |
| System exergy efficiency | 23.77% | | 28.08% | |

As can be seen from Table 3, considering the benefits of desalination and the BOG was liquefied and fed into the organic Rankine cycle power generation system in the new system scheme, the exergy efficiency of it is much higher than that of the original system. In order to further improve the exergy efficiency of the system, the pure fluid in the new system scheme will be replaced with the mixed working fluid to make the heat exchange curve of heat exchanger can be more matched.

## 3. Matching Research of Mixed Working Fluid for the New System Scheme

### 3.1 Proposal for mixed working fluid

From the analysis results in Table 3, the exergy loss of LHEX1, LHEX3 and WHEX3 in the new system scheme

(i.e., BOG recondensation LNG cold energy comprehensive utilization system) is greater. Figs. 2–4 show the heat exchange Temperature-Heat flow (*T-Q*) curves of LHEX1, LHEX3 and WHEX3 for LNG with pure working fluid, respectively.

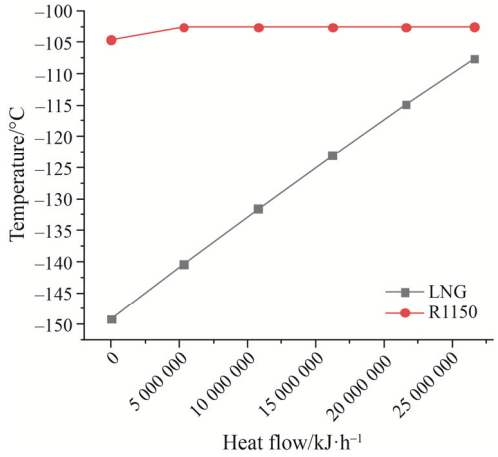


**Fig. 2** LHEX1 *T-Q* curve (pure working fluid)

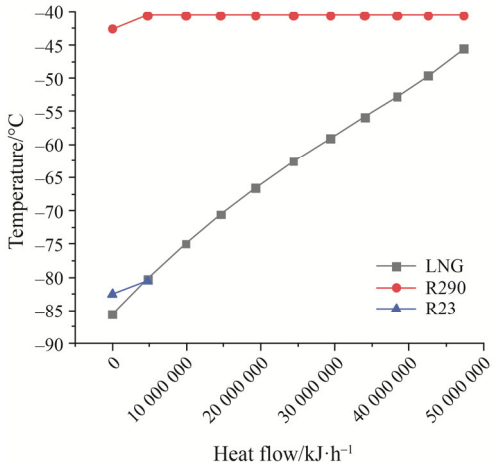


**Fig. 3** LHEX3 *T-Q* curve (pure working fluid)

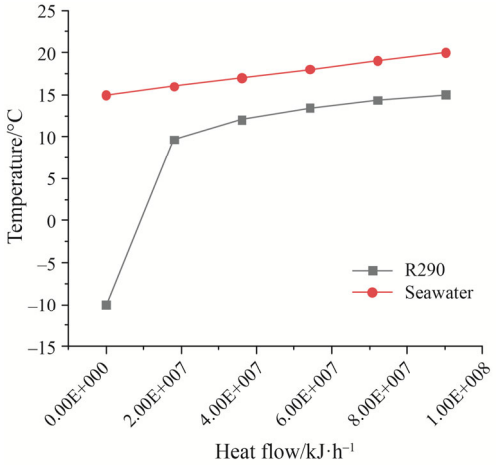


**Fig. 4** WHEX3 *T-Q* curve (pure working fluid)

As can be seen from the figure, the temperature difference of the heat exchanger is too large, and the temperature of the cold and heat flow does not match, resulting in a large heat transfer loss. It shows that there is room for improvement of the first and third stage circulating working fluid, while the second circulating medium remains unchanged. Because the cold liquid inlet temperature of LHEX1 is constant, in order to reduce the heat exchange loss, it is necessary to select a suitable non-azeotropic mixture working fluid to make the temperature change of circulating medium in LHEX1 closer to that of LNG. When the newly selected working fluid is mixed with the original working fluid, the saturation temperature of the new mixed working fluid in the same pressure should be lower than that of the original working fluid. In this way, when the first stage working fluid enters LHEX1, the temperature can be closer to LNG, so that the heat transfer curve of LHEX1 can be more matched. At present, the research on mixed working fluid is mainly classified as hydrocarbon mixed working fluid, refrigerant mixed working fluid and ammonia water mixture. Because R1150 belongs to refrigerant working fluid, it can be found that only R14 meets the conditions by comparing common working fluids. Mixing R14 with R1150, the R14 content in the mixed working fluid is from 0% to 100%, and the intermediate interval is 10%, which are RA0 (R1150), RA1 (R1150:R14=9:1), RA2 (R1150:R14=8:2), RA3, ..., RA10.

Similarly, it is necessary to select an appropriate mixture working fluid to make the temperature change of circulating medium in LHEX3 closer to that of LNG. Because R290 belongs to hydrocarbon working fluid, the mixing working fluid should also be hydrocarbons. It is found that only R170 meets the requirements. When R170 and R290 are mixed, the content of R170 in the mixed working fluid changed from 0% to 100%, and the interval of 10% changed in turn, namely RC0 (R290), RC1 (R290:R170=9:1), RC2 (R290:R170=8:2), RC3, ..., RC10.

For WHEX3, the heat source is seawater, and its temperature remains unchanged, and the cold source is the third stage circulating working fluid. In order to form an appropriate non-azeotrope mixture to adapt to the temperature matching of the two working media in WHEX3, through the analysis of the commonly used working media, it is found that only R600a meets the requirements. Similarly, when R600a and R290 are mixed, the content of R600a in mixing working fluid is from 0% to 100%. When the interval of 10% changes in turn, they are RB0 (R290), RB1 (R290:R600a=9:1), RB2 (R290:R600a=8:2), RB3, ..., RB10.

In summary, the first-stage mixed working fluid has the RA series; the second-stage working fluid is

unchanged, and the third-stage mixed working fluid has the RB and RC series. Therefore, the system working fluid matching scheme is shown in Supplementary Table S1.

Supplementary Table S1 shows a total of 200 possible combinations of working media, but it is found through simulation that when the proportion of the first-stage mixed working fluid R14 exceeds 20%, the circulating working fluid is not completely condensed in the LHEX1, resulting the working fluid entering the WFPP1 is accompanied by gas entering, affecting the operation of the system. Therefore, the first stage working fluids are only RA0, RA1, and RA2, which can make the system operate.

When the third-stage mixed working fluid is the RB series, once the R600a ratio exceeds 20%, it is not only mixed with gas in the working fluid of WFPP3, but also cause the temperature crossover phenomenon of the hot and cold flows in the WHEX4. The reason is that with the increase of R600a content, the temperature at the outlet of WFPP3 rises, further causing temperature crossover in WHEX4.

When the third-stage working fluid is RC series, once the R170 ratio exceeds 10%, the temperature crossover phenomenon occurs in the WHEX2, because of the dew point and the bubble point temperature of the mixed working fluid decrease as the R170 content increases. The heat flow temperature in the WHEX2 is condensed too low, causing a temperature crossover phenomenon, and finally, the third-stage mixed working fluid that can make the system operate normally is RB0, RB1, and RC1. Combined with the first-stage working fluid mentioned above, the working fluid combination for normal operation of the system is shown in Table 4.

**Table 4** Working fluid matching table for normal operation of system

| | Plan 1 | Plan 2 | Plan 3 | Plan 4 |
|---|---|---|---|---|
| First stage working fluid | RA0 | RA0 | RA1 | RA1 |
| Second stage working fluid | R23 | R23 | R23 | R23 |
| Third stage working fluid | RB0 | RB1 | RB0 | RB1 |
| | Plan 5 | Plan 6 | Plan 7 | Plan 8 |
| First stage working fluid | RA1 | RA2 | RA2 | RA2 |
| Second stage working fluid | R23 | R23 | R23 | R23 |
| Third stage working fluid | RC1 | RB0 | RB1 | RC1 |

### 3.2 Contrastive analysis of mixed working fluid schemes

According to the eight schemes in Table 4 mentioned above, a comparative analysis is given in terms of working fluid saturation pressure, gas fraction, net output power of the system, fresh water yield, exergy efficiency and economic benefits.

Fig. 5 shows the saturation pressure variation trend of the third-stage mixed working fluid with the heat source temperature of the system. Fig. 6 shows the variation trend of the gas fraction at the outlet of expander TB1 with the system heat source temperature.

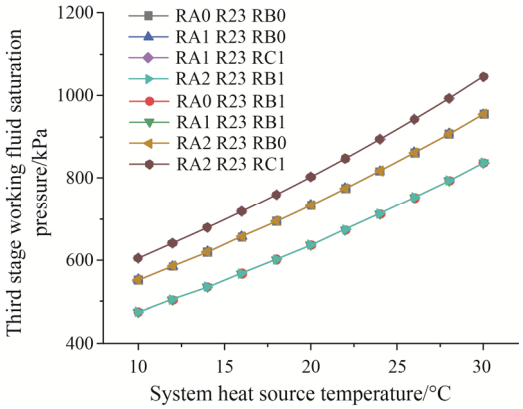


**Fig. 5** Variation of working fluid saturation pressure with system heat source temperature and working fluid mixing ratio

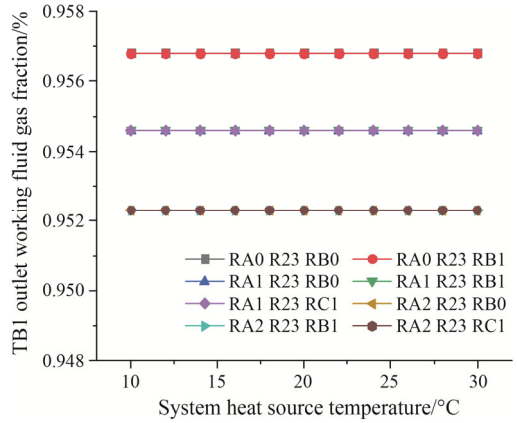


**Fig. 6** Vapor fraction at TB1 outlet varies with system heat source temperature and working fluid mixing ratio

From Fig. 5, when the third-stage working fluid is RC1, the saturation pressure is the highest, followed by RB0 and the RB1, and the saturation pressure of each mixture increases with the increase of the temperature after vaporization. The vaporization temperature is directly related to the system heat source temperature (i.e., seawater temperature). The higher the saturation pressure, the higher the temperature, the greater the output power of TB3, and the higher the net output power and efficiency of the system.

From Fig. 6, when the first working fluid is RA0, the gas fraction is the highest, followed by RA1, and RA2 is the lowest. The gas fraction of each mixed working fluid remains unchanged with the increase of the system heat source temperature, and the low fraction of the gas phase

also causes the liquid to enter the turbine, reduce turbine power and shorten turbine service life. Generally, the phenomenon will not be caused when the dryness is above 0.94.

Fig. 7 shows the variation trend of the gas fraction at the outlet of expander TB3 with the system heat source temperature. From Fig. 7, when the third working fluid is RB1, the gas fraction is the highest, followed by RB0, and RC1. The gas fraction of each working fluid increases with the system heat source temperature, and there is no liquid hammer.

Fig. 8 shows the changing trend of system net output power with different mixed working fluid and the heat source temperature. Fig. 9 shows the changing trend of seawater desalination with different working fluid and system heat source temperature.

From Fig. 8, it can be seen from the graph that when the temperature of the heat source is 10°C to 30°C, the system net output power is the highest when the working fluids are RA1, R23 and RC1, and it increases with the increase of the heat source temperature. When the mixtures are RA2, R23 and RB1, the net output power of the system is the lowest.

From Fig. 9, it can be seen from the chart that the amount of seawater desalination is related to the third working fluid. When the third working fluid is RC1, the amount of seawater desalination is the highest, followed by RB0 and RB1. When the third working fluid is RC1 and RB0, the desalination capacity remains unchanged with the increase of heat source temperature. When the working fluid is RB1, the desalination capacity continues to decrease with the increase of heat source temperature.

Fig. 10 shows the changing trend of system exergy efficiency with different working fluid and the heat source temperature. Fig. 11 shows the changing trend of system economic benefit of different working fluid and the heat source temperature.

From Fig. 10, it can be seen from the figure that when the heat source temperature is 10°C to 30°C, and the working fluid is RA1, R23 and RC1, the system has the highest exergy efficiency, followed by RA2, R23 and RC1. When the working fluid is RA2, R23 and RB1, the

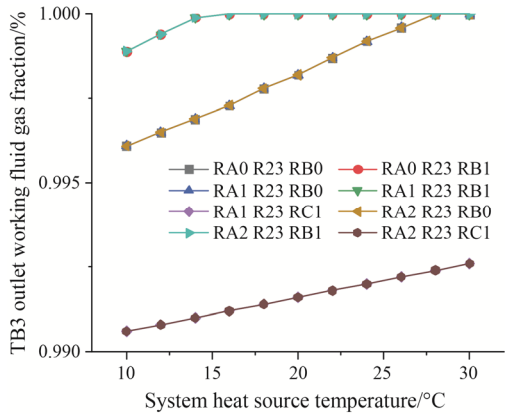


**Fig. 7** Vapor fraction at TB3 outlet varies with system heat source temperature and working fluid mixing ratio

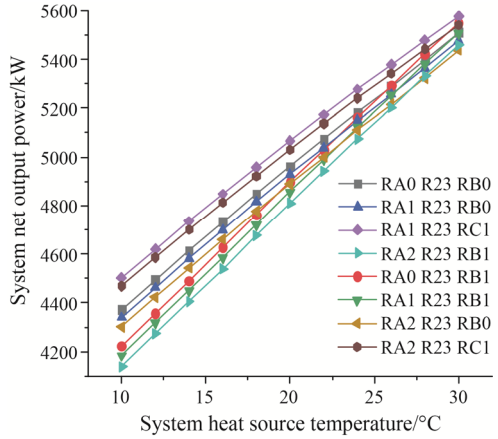


**Fig. 8** The system net output power varies with the system heat source temperature and working fluid mixing ratio

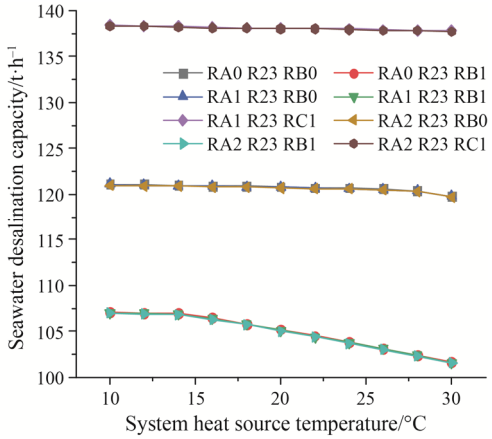


**Fig. 9** The variation of desalination capacity with the system heat source temperature and working fluid mixing ratio

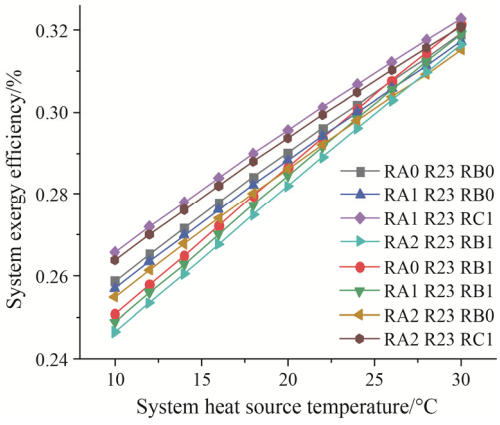


**Fig. 10** The system exergy efficiency varies with the system heat source temperature and working fluid mixing ratio

system has the lowest exergy efficiency. Moreover, the system exergy efficiency increases with the increase of heat source temperature.

From Fig. 11, it can be seen that when the heat source temperature is 10°C to 30°C, and the working fluid is RA1, R23 and RC1, the system has the highest economic benefit; RA2, R23 RC1 is the second. When the working fluid is RA2, R23 and RB1, the system has the lowest economic efficiency. The system economic benefits of different working fluid increase with the increase of heat source temperature.

Supplementary Figs. S3–S5 show the heat exchange *T-Q* curves of heat exchange between LNG and mixed working fluid in LHEX1, LHEX3 and WHEX3. Compared with Figs. 2–4, it can be found that the heat transfer curve of the heat exchanger is more matched when the mixed working fluid is used, to achieve the purpose of reducing heat transfer exergy loss and improving the exergy efficiency.

Fig. 12 shows the heat exchange exergy losses of LHEX1, LHEX3 and WHEX3 in the pure working fluid and mixed working fluid. It can be found that the heat exchange exergy losses of mixed working fluid are significantly smaller than that of pure working fluid.

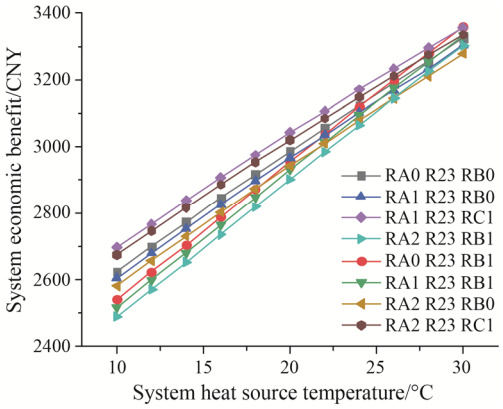


**Fig. 11** The system economic benefit varies with the system heat source temperature and working fluid mixing ratio

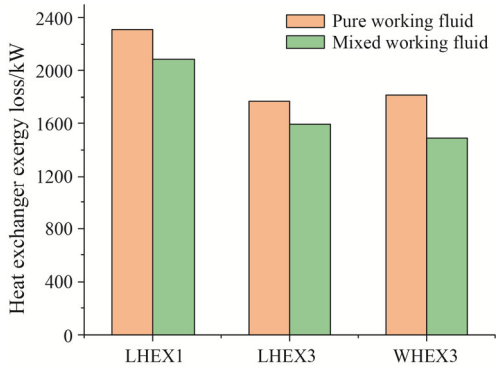


**Fig. 12** Comparison of heat transfer exergy losses between pure and mixed working fluid

In conclusion, the RA1, R23 and RC1 combination schemes are superior to other working fluid combination schemes in terms of net output power, exergy efficiency and system economic benefits. The system exergy efficiency of the mixed working fluid combination is 29.56%, and compared with the original pure working fluid, the combination increased by 5.27%.

## 4. Parameter Optimization of the New System Scheme

### 4.1 Influence of single parameter change on the new system

A good LNG cold energy utilization system not only requires a reasonable process planning and combination of working fluids, but also requires optimal matching of system parameters. After optimization of process planning and working fluid, the core of the new system scheme is three-stage longitudinal organic Rankine cycle power generation system. Moreover, the temperature of working fluid at all levels in the system corresponds to the condensation pressure one by one, and adjusting the pressure of working fluid at all levels will affect the whole system. Therefore, the following single variable simulation is conducted to obtain the influence of condensation pressure of the organic Rankine cycle working fluid at all levels on the net output power and desalination capacity of the system. The results are shown in Fig. 13.

It can be seen from Fig. 13 that the system net output power and seawater desalination increase with the increase of the first-stage working fluid condensing pressure, and decrease with the decrease of the second-stage working fluid condensing pressure. For the third working fluid, the net output power of the system first increases with the increase of the third working fluid condensation pressure, and then decreases with the increase of condensation pressure that the working fluid after exceeding a critical point. The seawater desalination capacity decreases with the increase of the third working fluid condensation pressure.

Based on the above analysis, it is found that the condensation pressure of organic Rankine cycle working fluid have a great influence on the net output power and desalination capacity of the system, and they are coupled and superimposed on the system as a whole. Therefore, the single control variable method can't effectively optimize the whole system, and it is necessary to perform multi-point global optimization on the system.

### 4.2 Proposition of genetic algorithm

The genetic algorithm simulates the characteristics of biological inheritance, which can combine multiple variables into one initial population by coding, and then

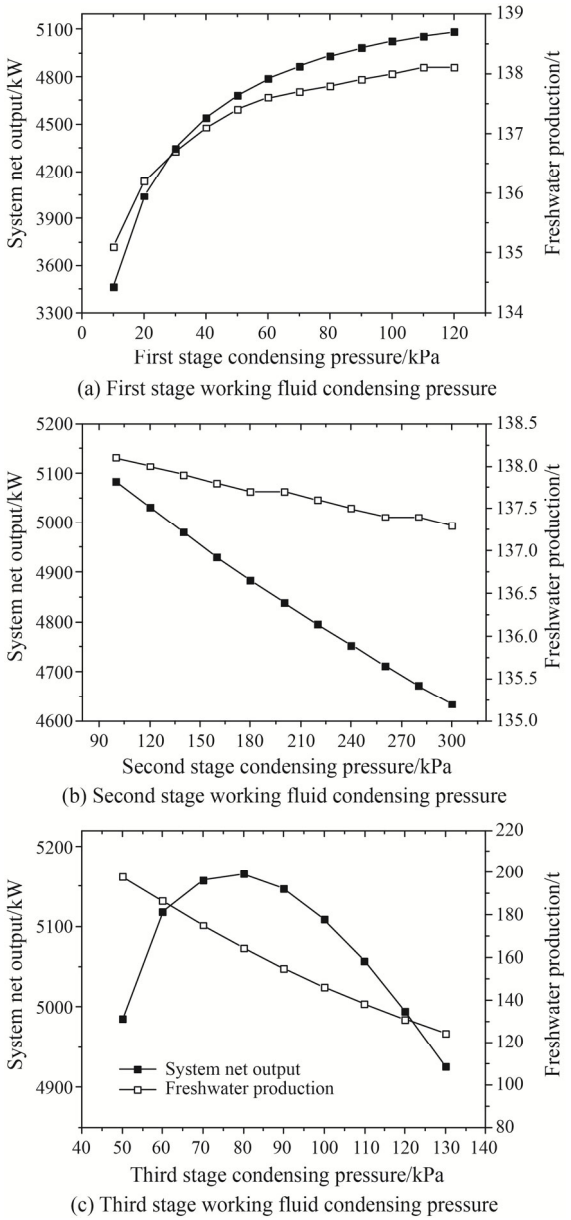


**Fig. 13** Curve of network and fresh water volume of the system with the condensing pressure of working fluid at different levels

achieves the evolutionary process of survival of the fittest through genetic iteration. It has good global search ability [27].

As an evaluation criterion, different objective functions correspond to different standard, and their corresponding optimization results are also different. In this paper the system total exergy efficiency is selected as the objective function to optimize the system.

Total system exergy efficiency is expressed as

$$\max F = \eta = \frac{\sum_{i=1}^{3} W_i + W_j - \sum_{k=1}^{6} P_k}{Ex_{\mathrm{LNG}} + Ex_{\mathrm{seawater}}} \tag{3}$$

where $W_i$ is the turbine output power; $W_j$ is the seawater desalination yield; $P_k$ is the power consumption of each pump of the system; $Ex_{\mathrm{LNG}}$ is the exergy of the LNG entering the system; $Ex_{\mathrm{seawater}}$ is the exergy value of the seawater entering the system.

### 4.3 Optimization parameters and constraints

Based on the above analysis, the optimal optimization parameters of the system are determined as three-stage working fluids condensation pressure.

First of all, the parameter optimization interval should ensure that the parameters in this interval make the system operate normally, and there is no temperature crossover phenomenon. The LNG logistics exported from LHEX3 is used for desalination of seawater, which belongs to low-grade cold energy, and its temperature should not be higher than –40°C. The corresponding third working fluid condensation pressure should not exceed 120 kPa. The LHEX1 outlet LNG temperature should not be higher than –106°C; otherwise it will cause the LHEX3 temperature to cross, and the corresponding first-stage working fluid condensing pressure should not exceed 130 kPa. The LHEX2 outlet LNG temperature should not exceed –51°C; otherwise, WHEX2 will cause temperature crossover, and the corresponding second-stage working fluid condensation pressure can't exceed 460 kPa. Under the premise of ensuring the system normal operation, the minimum condensation pressure of the first, the second and the third medium is 10 kPa, 10 kPa and 54 kPa. In summary, the optimization intervals of each parameter are shown in Table 5.

**Table 5** Optimum intervals of parameters

| Parameter | Lower limit | Upper limit |
|---|---|---|
| First level condensation pressure/kPa | 10 | 130 |
| Second level condensation pressure/kPa | 10 | 460 |
| Third level condensation pressure/kPa | 54 | 120 |

### 4.4 Fitness function

In genetic algorithm programming, the individual adaptive function is usually used to adjust the group structure and evolution, so the adaptive function is very important. When a new generation of the population is generated, each individual in the old population is copied proportionally into the next generation according to the size of the fitness function value, and the individuals with large fitness function value are more likely to enter the next generation of evolution [28]. The optimal solution of the LNG cold energy multi-level utilization system of the FSRU platform designed in this paper is the maximum value of the objective function. Based on a general

fitness function proposed in Ref. [29], this paper adjusts the fitness function according to the actual situation of system optimization. The fitness function is as follows.

$$\mathrm{Fit}\left[f(x)\right]=1-0.5\left[\left|\frac{f(x)-b}{\alpha^{1.2}}\right|\right]^{\alpha},\left|f(x)-b\right|<\alpha \quad (4)$$

$$\mathrm{Fit}\left[f(x)\right]=\frac{1}{1+\left[\left|\frac{f(x)-b}{\alpha}\right|\right]^{\beta}},\left|f(x)-b\right|\geq\alpha \quad (5)$$

Usually, $b$ is the objective function value, i.e., $b$=max$f(x)$; the initial exergy efficiency of the system is 29.56%; the initial $b$ value is 0.3; the $\beta$ value is 2; the initial value of the $\alpha$ is 1, and the fitness value at [0.3, 1] is linear, and the late $\alpha$ value is 0.5, because the function changes slowly near the global optimal solution max $f(x)$; using $\alpha$=0.5 can make the fitness function flexibly reflect the change of the target value. It is more favorable for future choices. In the iteration process, the $b$ value takes the maximum value after each iteration, and $\alpha$ is adjusted by Eq. (6).

$$\alpha=\max\left[0.5,\frac{\left|\max f_i-\min f_i\right|}{30}\right] \quad (6)$$

where max $f_i$ and min $f_i$ are the maximum and minimum values of the $i$-th generation.

### 4.5 Optimization results and analysis

With the total system exergy efficiency as the objective function, the condensation pressure of all working fluids in the power generation part is optimized by a genetic algorithm. After several iterations, the optimized values of the parameters with the system exergy efficiency as the objective function are shown in Table 6. More detailed optimization data comparison is shown in Table 7.

According to the data in Table 7, the exergy loss of the system after optimization is 11 759 kW, which is 2.6% lower than that before optimization. The net output power of the system is 5186 kW, and the efficiency is 30.6%, which are 2.36% and 3.51% higher than that before optimization.

### 4.6 System economic benefit analysis

According to the inquiry of China's domestic market, the total estimated investment value of the initial input equipment of the system is given in Supplementary Table S2.

It can be seen from Supplementary Table S2 that the estimated equipment investment for the final optimized design system. The total investment cost of the system is given by the following formula [30].

$$C_{\mathrm{total}}=\sum_k\left(Z_{\mathrm{CI}}+Z_{\mathrm{OM}}\right)_k \quad (7)$$

where, $Z_{\mathrm{CI},k}$ is the investment cost of system components, $Z_{\mathrm{OM},k}$ is the operation and maintenance cost of the system.

$$Z_{\mathrm{CI},k}+Z_{\mathrm{OM},k}=\frac{Z_k\cdot\Phi}{N\cdot3600}\mathrm{CRF} \quad (8)$$

where, $Z_k$ is the investment cost of each component of the system; $\Phi$ is the system maintenance coefficient, taking 1.06 [31]; $N$ is the annual operation time of the system, taking 7300 hours [32], and the capital recovery factor (CRF) is defined as follows:

$$\mathrm{CRF}=\frac{i(1+i)^n}{(1+i)^n-1} \quad (9)$$

where, $n$ is the system lifetime, taking 20 years [33]; $i$ is the annual interest rate, taking 14% [31]. The electricity production cost (EPC) and the annual total net income (ATNI) of the system are given as follows, respectively [34].

$$\mathrm{EPC}=\frac{3600C_{\mathrm{total}}}{W_{\mathrm{net}}} \quad (10)$$

**Table 6** Parameter values before and after optimization

| | First level condensation pressure/kPa | Second level condensation pressure/kPa | Third level condensation pressure/kPa |
|---|---|---|---|
| Before optimization | 110 | 110 | 110 |
| After optimization | 129 | 115 | 81 |

**Table 7** Data comparison before and after system parameter optimization

| Module | Before system optimization | | After system optimization | |
|---|---|---|---|---|
| | Exergy loss/kW | Exergy efficiency | Exergy loss/kW | Exergy efficiency |
| Organic Rankine cycle power generation | 10 243 | 27.17% | 9335 | 28.46% |
| Seawater desalination | 1446 | 46.26% | 2021 | 42.11% |
| BOG processing | 383 | 82.40% | 392 | 82.00% |
| System total exergy loss/kW | 12 073 | | 11 759 | |
| System net output power/kW | 5066 | | 5186 | |
| System exergy efficiency | 29.56% | | 30.60% | |
| System working fluid | R1150, R23, R290, R600a | | R1150, R23, R290, R600a | |

$$\mathrm{ATNI} = 7300\left(\mathrm{EP} - \mathrm{EPC}\right)\cdot W_{\mathrm{net}} \tag{11}$$

where, EP is the current electricity price, taking 0.86 CNY/(kW·h) (the data comes from China's industrial electricity sales prices). EPC is the unit power production cost of the system (taking the system life as 20 years), and the calculated EPC value is 0.148 CNY. The difference between these two is the system net profit of power production per unit. Through the above formula, the annual total net income of the system can be calculated is 18.71 million CNY.

## 5. Conclusions

Taking a certain FSRU of the LNG vaporization volume of 175 t/h as the object, a comprehensive utilization system of cold energy from LNG vaporization considering BOG processes was studied. Through the simulation and optimization design of the system, the following conclusions are obtained:

(1) In the single-split longitudinal three-stage organic Rankine cycle power generation with direct-freezing seawater desalination system coupled with BOG recondensation processing technology, the pure working fluids for three-stage organic Rankine cycle that best match the system are R1150, R23 and R290, and the intermediate medium of seawater desalination is R600a.

(2) Based on the comparative analysis of the influence of pure working fluid and eight kinds of mixed working fluid on the performance of BOG recondensation LNG cold energy comprehensive utilization system, the optimal combination of mixture working fluid in the three-stage circulating system was selected as follows: RA1 (R1150:R14=9:1) for first stage, R23 for second stage, RC1 (R290:R170=9:1) for third stage. The optimum condensation pressures of the first, second and third working fluid in the new system are 129 kPa, 115 kPa and 81 kPa, respectively.

(3) The optimization results show that the exergy efficiency of the BOG recondensation LNG cold energy comprehensive utilization system is 30.6%, and the system economic benefit is 18.71 million CNY per year.

(4) The system scheme can effectively improve the utilization efficiency of the LNG cold energy of the system, and provides technical support for the design optimization and application of the cold energy comprehensive utilization system on the LNG-FSRU platform. However, the overall efficiency of the system still needs to be improved. In the later stage, the heat source generated by other equipment on the LNG-FSRU can be recycled and combined with seawater to provide a variety of heat sources for the system, so as to further improve the energy utilization rate of the system.

## Acknowledgements

This research was supported by special project of R&D and industrialization of Marine equipment of national development and reform commission of China (National Development and Reform Commission High Technology [2015] No.1409)

## References

[1] Fahmy M., Nabih H., Impact of ambient air temperature and heat load variation on the performance of air-cooled heat exchangers in propane cycles in LNG plants—analytical approach. Energy Conversion and Management, 2016, 121: 22–35.

[2] Fahmy M., Nabih H., El-Rasoul T., Optimization and comparative analysis of LNG regasification processes. Energy, 2015, 91: 371–385.

[3] Uwitonze H., Han S., Jangryeok C., Hwang K., Design process of LNG heavy hydrocarbons fractionation: Low LNG temperature recovery. Chemical Engineering and Processing: Process Intensification, 2014, 85: 187–195.

[4] Lee I., Park J., Moon I., Conceptual design and exergy analysis of combined cryogenic energy storage and LNG regasification processes: cold and power integration. Energy, 2017, 140: 106–115.

[5] Franco A., Casarosa C., Thermodynamic analysis of direct expansion configurations for electricity production by LNG cold energy recovery. Applied Thermal Engineering, 2015, 78: 649–657.

[6] Xue F., Chen Y., Ju Y., A review of cryogenic power generation cycles with liquefied natural gas cold energy utilization. Energy Procedia, 2016, 10: 363–374.

[7] Angelino G., Invernizzi C., The role of real gas Brayton cycles for the use of liquid natural gas physical exergy. Applied Thermal Engineering, 2011, 31: 827–833.

[8] Prananto L., Zaini I., Mahendranata B., Juangsa F., Aziz M., Soelaiman T., Use of the Kalina cycle as a bottoming cycle in a geothermal power plant: Case study of the Wayang Windu geothermal power plant. Applied Thermal Engineering, 2018, 132: 686–696.

[9] Sun X., Yao S., Xu J., Feng G., Yan L., Design and optimization of a full-generation system for marine LNG cold energy cascade utilization. Journal of Thermal Science, 2020, 29(3): 587–596.

[10] Le S., Lee J., Chen C., Waste cold energy recovery from liquefied natural gas (LNG) regasification including pressure and thermal energy. Energy, 2018, 152: 770–787.

[11] Bao J., Lin Y., Zhang R., Zhang N., He G., Strengthening power generation efficiency utilizing liquefied natural gas cold energy by a novel two-stage condensation Rankine

cycle (TCRC) system. Energy Conversion and Management, 2017, 143: 312–325.

[12] Bao J., Lin Y., Zhang R., Zhang N., He G., Effects of stage number of condensing process on the power generation systems for LNG cold energy recovery. Applied Thermal Engineering, 2017, 126: 566–582.

[13] Zhao L., Dong H., Tang J., Cai J., Cold energy utilization of liquefied natural gas for capturing carbon dioxide in the flue gas from the magnesite processing industry. Energy, 2016, 105: 45–46.

[14] Salem A., Hudiab E., LNG regasification system to enhance the performance of gas turbines and water desalination systems. International Journal of energy, 2014, 8: 84–90.

[15] Mehrpooya M., Esfilar R., Moosavian S., Introducing a novel air separation process based on cold energy recovery of LNG integrated with coal gasification, transcritical carbon dioxide power cycle and cryogenic $CO_2$ capture. Journal of Cleaner Production, 2017, 142: 1749–1764.

[16] Liu B., Rivière P., Coquelet C., Gicquel R., David F., Investigation of a two stage Rankine cycle for electric power plants. Applied Energy, 2012, 100: 285–294.

[17] Zhang M., Zhao L., Liu C., Cai Y., Xie X., A combined system utilizing LNG and low-temperature waste heat energy. Applied Thermal Engineering, 2016, 101: 525–536.

[18] Sun H., Zhu H., Liu F., Ding H., Simulation and optimization of a novel Rankine power cycle for recovering cold energy from liquefied natural gas using a mixed working fluid. Energy, 2014, 70: 317–324.

[19] Yao S.G., Tang L., Xu L.K., Feng G.Z., A supercritical single split longitudinal three-stage Rankine cycle power generation system. China, 2018, CN201710904258.8.

[20] Yao S.G., Xu L.K., Tang L., New cold-level utilization scheme for cascade three-level Rankine cycle using the cold energy of liquefied natural gas. Thermal Science, 2019, 23: 3865–3875.

[21] Yoonho L., LNG-FSRU cold energy recovery regasification using a zeotropic mixture of ethane and propane. Energy, 2019, 173: 857–869.

[22] Zhang G., Li B., Zhang X., Wang Q., Design and simulation analysis of cold energy utilization system of LNG floating storage regasification unit. Earth and Environmental Science, 2019, 300: 022117.

[23] Rao H., Karimi I., Optimal design of boil-off gas reliquefaction process in LNG regasification terminals. Computers & Chemical Engineering, 2018, 117: 171–190.

[24] Wu M., Zhu G., Sun D., He J., Optimization model and application for the recondensation process of boil-off gas in a liquefied natural gas receiving terminal. Applied Thermal Engineering, 2019, 147: 610–622.

[25] Zhang C., Pan Z., Shang L Y., Yang F., BOG treatment process optimization and energy consumption analysis of LNG receiving station. Oil and gas storage and transportation, 2017, 4: 421–425.

[26] Williams P.M., Ahmad M., Connolly B.S., Oatley-Radcliffe D.L., Technology for freeze concentration in the desalination industry. Desalination, 2015, 356: 314–327.

[27] Boulougouris E.K., Papanikolaou A.D., Multi-objective optimisation of a floating LNG terminal. Ocean Engineering, 2008, 35: 787–811.

[28] Mokshin A., Mokshin V., Sharnin L., Adaptive genetic algorithms used to analyze behavior of complex system. Communications in Nonlinear Science and Numerical Simulation, 2019, 71: 174–186.

[29] Chen Q., Worden K., Peng P., Genetic algorithm with an improved fitness function for (N)ARX modelling. Mechanical Systems and Signal Processing, 2007, 21: 994–1007.

[30] Lee S., Choi B., Thermodynamic assessment of integrated heat recovery system combining exhaust-gas heat and cold energy for LNG regasification process in FSRU vessel. Journal of mechanical science and technology, 2016, 30(3): 1389–1398.

[31] Mosaffa A.H., Farshi L.G., Exergoeconomic and environmental analyses of an air conditioning system using thermal energy storage. Applied Energy, 2016, 162: 515–526.

[32] Mosaffa A.H., Mokarram N.H., Farshi L.G., Thermo-economic analysis of combined different ORCs geothermal power plants and LNG cold energy. Geothermics, 2017, 65: 113–125.

[33] Choi I., Lee S., Seo Y., Chang D., Analysis and optimization of cascade Rankine cycle for liquefied natural gas cold energy recovery. Energy, 2013, 61: 179–195.

[34] Bao J., Lin Y., Zhang R., Zhang N., He G., Effects of stage number of condensing process on the power generation systems for LNG cold energy recovery. Applied Thermal Engineering, 2017, 126: 566–582.

## Supplementary Data

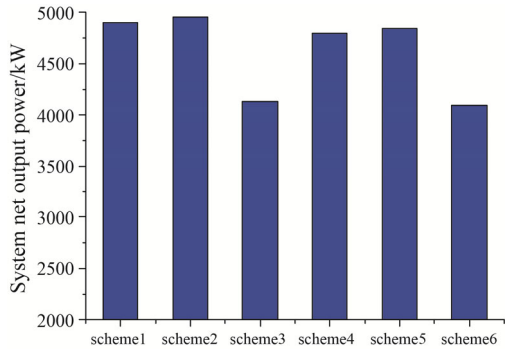


**Fig. S1** Net output power for each scheme of working fluid combination

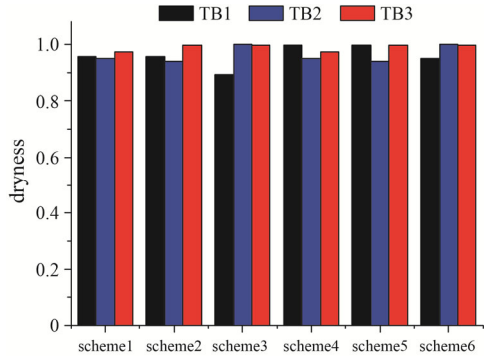


**Fig. S2** Working fluid dryness at the three turbine outlets for each scheme of working fluid combination

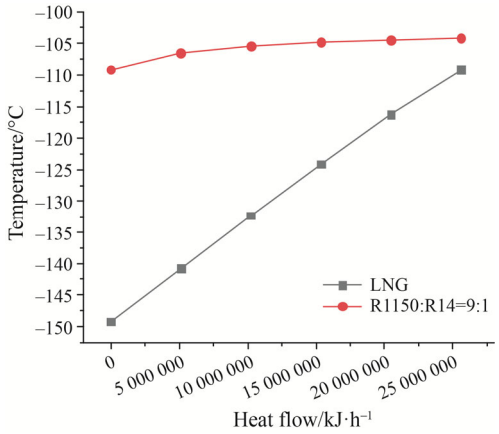


**Fig. S3** LHEX1 *T-Q* curve (mixed working fluid)

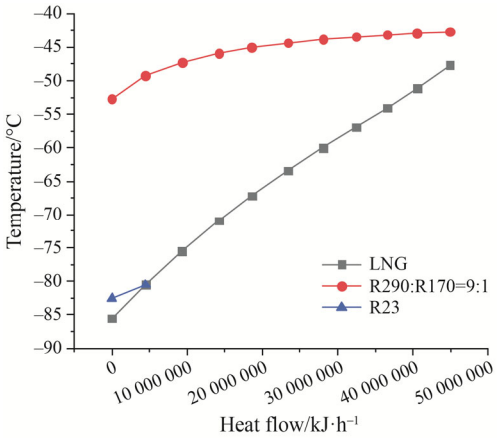


**Fig. S4** LHEX3 *T-Q* curve (mixed working fluid)

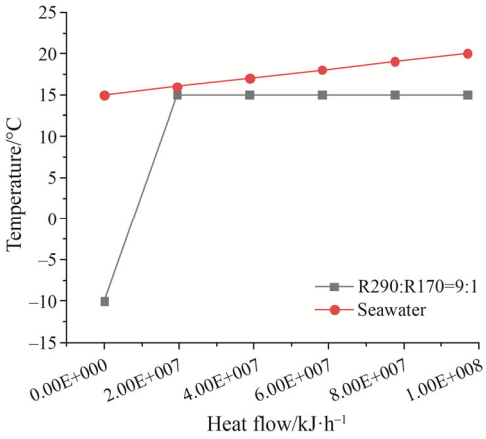


**Fig. S5** WHEX3 *T-Q* curve (mixed working fluid)

**Table S1** Theoretical working fluid matching table

| First stage working fluid | Second stage working fluid | Third stage working fluid | First stage working fluid | Second stage working fluid | Third stage working fluid |
|---|---|---|---|---|---|
| RA0 | R23 | RB0-RB10, RC0-RC10 | RA6 | R23 | RB0-RB10, RC0-RC10 |
| RA1 | R23 | RB0-RB10, RC0-RC10 | RA7 | R23 | RB0-RB10, RC0-RC10 |
| RA2 | R23 | RB0-RB10, RC0-RC10 | RA8 | R23 | RB0-RB10, RC0-RC10 |
| RA3 | R23 | RB0-RB10, RC0-RC10 | RA9 | R23 | RB0-RB10, RC0-RC10 |
| RA4 | R23 | RB0-RB10, RC0-RC10 | RA10 | R23 | RB0-RB10, RC0-RC10 |
| RA5 | R23 | RB0-RB10, RC0-RC10 | | | |

**Table S2** Estimation of system equipment investment cost (equipment unit price from China network inquiry)

| Equipment | Unit Price/$10^5$ CNY | Number | Total/$10^4$ |
|---|---|---|---|
| LNG heat exchanger | 10 | 5 | 500 |
| Working fluid heat exchanger | 5 | 4 | 200 |
| LNG-BOG heat exchanger | 5 | 2 | 100 |
| LNG pressure pump | 20 | 1 | 200 |
| Working fluid pump | 5 | 4 | 200 |
| Seawater pump | 15 | 2 | 300 |
| Turbine | 25 | 3 | 750 |
| BOG compressor | 5 | 1 | 50 |
| Desalination equipment | 100 | 1 | 1000 |
| Circulating pipe | 1000 CNY/m | 2000 | 200 |
| Total | | | 3500 |